Acta Oceanol. Sin., 2019, Vol. 38, No. 5, P. 76–85
https://doi.org/10.1007/s13131-019-1441-3
http://www.hyxb.org.cn
E-mail: hyxbe@263.net

Asymmetric response of the eastern tropical Indian SST to climate warming and cooling

Shan Xu[1, 2], Yiyong Luo[2]*, Fukai Liu[1, 2]

[1] College of Oceanic and Atmospheric Sciences, Ocean University of China, Qingdao 266100, China

[2] Physical Oceanography Laboratory, Ocean University of China, Qingdao 266100, China

Received 25 January 2018; accepted 2 March 2018

Abstract

The response of the eastern tropical Indian Ocean (ETIO) to heat fluxes of equal amplitude but opposite sign is investigated using the Community Earth System Model (CESM). A significant positive asymmetry in sea surface temperature (SST) is found over the ETIO—the warming responses to the positive forcing exceeds the cooling to the negative forcing. A mixed layer heat budget analysis is carried out to identify the mechanisms responsible for the SST asymmetry. Results show that it is mainly ascribed to the ocean dynamical processes, including vertical advections and diffusion. The net surface heat flux, on the contrary, works to reduce the asymmetry through its shortwave radiation and latent heat flux components. The former is due to the nonlinear relationship between SST and cloud, while the latter is resulted mainly from Newtonian damping and air-sea stability effects. Changes in the SST skewness are also evaluated, with more enhanced negative SST skewness over the ETIO found for the cooling than heating scenarios due to the asymmetric thermocline-SST feedback.

Key words: tropical Indian Ocean, SST asymmetry, climate warming, climate cooling, negative SST skewness

Citation: Xu Shan, Luo Yiyong, Liu Fukai. 2019. Asymmetric response of the eastern tropical Indian SST to climate warming and cooling. Acta Oceanologica Sinica, 38(5): 76–85, doi: 10.1007/s13131-019-1441-3

1 Introduction

The Indian Ocean dipole (IOD) is an intrinsic ocean–atmosphere coupled mode over the tropical Indian Ocean on interannual time scales and is usually phase-locked to austral spring (Saji et al., 1999; Webster et al., 1999). This dipole mode has a positive phase (pIOD) and a negative phase (nIOD). A pIOD (nIOD) event is featured with cold (warm) SST anomalies over the eastern tropical Indian Ocean (ETIO) but warm (cold) SST anomalies over the western tropical Indian Ocean (WTIO), accompanied with easterly (westerly) anomalies of surface winds along the equatorial Indian Ocean. It has great impacts on regional and global climate (Saji and Yamagata, 2003), like droughts in southeast Australia (Cai et al., 2009), rainfall in South America (Chan et al., 2008) and East Africa (Behera et al., 2005) and Indian summer monsoon (Ashok et al., 2004).

Previous studies (Hong et al., 2008, 2010; Cai and Qiu, 2013) found, over the ETIO region, the cold SST anomalies during the pIOD events are able to grow larger than the warm SST anomalies during the nIOD events, and this SST anomaly asymmetry is referred as the negative SST skewness. The formation processes responsible for the negative SST skewness are still a contentious issue. Several possible mechanisms have been proposed, including the nonlinear ocean temperature advection (Hong and Li, 2008; Hong et al., 2010; Cai and Qiu, 2013), the asymmetric thermocline-SST feedback as a part of the Bjerknes loop (Zheng et al., 2010; Ogata et al. 2013; Cai and Qiu, 2013), and the asymmetric SST-cloud-radiation feedback (Hong et al., 2008, 2010). For example, Hong et al. (2008) found that the nonlinear ocean temperature advective process assists to reinforce cold anomalies in the positive events but damp the warm anomalies in the negative events. Zheng et al. (2010) proposed that the asymmetric thermocline-SST feedback is a main driver in generating the negative SST skewness in ETIO: the surface warming induced by subsurface thermocline shoaling is more effective than the cooling resulted from a deepening thermocline, as the mean thermocline in the ETIO is deep. This hypothesis was further verified by Cai and Qiu (2013) and Ng et al. (2014a). Hong and Li (2010) argued that the thermocline feedback itself has little contribution and the skewness comes from a greater damping during nIOD than pIOD due to a breakdown of the SST-cloud-radiation feedback. In more details, during pIOD events the cold SST anomalies in the ETIO decrease cloud cover and atmospheric convection, allowing more incoming shortwave radiation, which in turn dampens the initial cooling. When cold SST anomalies in the ETIO drops to a threshold value, the breakdown occurs, leading to cloud-free conditions. Under this situation, the cold SST anomalies are able to grow freely since the anomalous atmospheric convection and incoming radiation remain constant.

Furthermore, studies have also suggested that the climatological mean state over the tropical Indian Ocean could to some extent alter the IOD frequency as well as the negative SST skewness. Under global warming, for instance, although IOD variance or amplitude has little changes (Zheng et al., 2010), the moderate pIOD events become more extreme (Ng et al., 2014b) and the frequency of extreme pIOD events increases by nearly three times because of the mean state change (Cai et al., 2014). Over the

Foundation item: The National Natural Science Foundation of China under contract No. 41676002; the Strategic Priority Research Program of the Chinese Academy of Sciences under contract No. XDA11010302.
*Corresponding author, E-mail: yiyongluo@ouc.edu.cn

ETIO, the negative SST skewness weakens by nearly 40% as the shoaling thermocline enhances the thermocline-SST feedback (Zheng et al., 2013). Furthermore, Cowan et al. (2014) found that this negative SST skewness is further enhanced during aerosol forcing than greenhouse gases (GHG) forcing. Therefore, it is important to examine how the mean states over the tropical Indian Ocean will change in response to different external forcings.

Recent studies have found significant changes of the tropical Indian Ocean under both GHG and aerosol forcings, with the former inducing a pIOD-like pattern (Luo et al., 2016) but the latter a nIOD-like pattern (Dong and Zhou, 2014; Cowan et al., 2014). In addition, there exists an asymmetry in the amplitude of SST changes over the ETIO, where the cooling responding to aerosol forcing exceeds the warming to GHG forcing (Li and Luo, 2018). These above conclusions on the tropical Indian Ocean are obtained from simulations with the historical anthropogenic GHG forcing and aerosol single forcing, in which the energy fluxes into the atmosphere-ocean coupled system are opposite in sign but not equal in amplitude, it is still not clear that whether this asymmetry is resulted from the asymmetric amplitude of the energy flux forcing between GHG and aerosols. In response to the uniform heating and cooling of equal amplitude energy heat fluxes, a zonal dipole asymmetric SST pattern is found in the equatorial Pacific Ocean with a positive anomaly in the east but a negative anomaly in the west (Liu et al., 2017). However, the mean climate and its variability are quite different between the tropical Pacific and tropical Indian, such as, the leading interannual mode is ENSO for the former but it is IOD for the latter. In addition, their responses to climate forcings also have significant differences. Under global warming, for example, the tropical Pacific SST is featured with an El Niño-like warming pattern with the ocean dynamics being its leading formation process (e.g., Luo et al., 2015, 2017), while the tropical Indian SST is characterized by a pIOD-like warming pattern with the Bjerknes feedback being its leading formation process (e.g., Zheng et al., 2013; Luo et al., 2016). Given these significant differences between the two basins as described above, it is important to understand the distinct signatures of response over the tropical Indian Ocean under climate warming and cooling. In this study, we employ NCAR's Community Earth System Model (CESM) and impose heat fluxes of equal amplitude but opposite sign into the ocean surface to examine the response of the tropical Indian Ocean to heating and cooling.

As will be shown later, asymmetric changes appears in many of surface and subsurface fields in the tropical Indian Ocean, thus, our main purpose of this study is to investigate the nonlinearity of the tropical Indian Ocean mean state in response to external forcings as well as its maintaining mechanisms. The rest of this paper is organized as follows. Section 2 briefly describes the models and simulations. Section 3 introduces the asymmetric changes over the tropical Indian Ocean under climate warming and cooling. Section 4 conducts a mixed layer heat budget analysis to examine the relative role of oceanic advection, diffusion, and air-sea heat flux for the SST asymmetry in the tropical Indian Ocean. Section 5 examines the underlying mechanisms that cause the negative SST skewness over the ETIO. Finally, a summary is given in Section 6.

2 Model and experiment design

The model employed by this study is CESM1.1, which is composed of Community Atmospheric Model Version 5 (CAM5), the Community Land Model Version 4 (CLM4) and the Parallel Ocean Program Version 2 (POP2). Three sets of experiments are designed with various degrees of complexity: the fully coupled, the slab ocean, and the partially coupled overriding experiments. For the fully coupled experiments in which all the model components are active, we first integrate an unforced control experiment (CTRL, Table 1) for 250 a. Then, two perturbation experiments, which are labeled HEAT and COOL (Table 1), are integrated for 250 a by adding and subtracting a uniform heat flux of 6 W/m^2 into the ocean surface, respectively. Results presented below are averaged over the last 100 a, and the sum of the anomalies in the two perturbation runs is used to quantify their asymmetry.

For the slab ocean experiments, we disable the ocean dynamics via employing a motionless slab ocean model (SOM). A control run (CTRL_SOM, Table 1) is integrated for 75 a with ocean heat transport fixed at a repeating annual cycle derived from CTRL. Branching out at the 51th year of the CTRL_SOM, HEAT_SOM and COOL_SOM (Table 1) are then integrated for 25 a with a uniform heat flux of 6 W/m^2 added into and extracted from the ocean, respectively. Therefore, the relative contribution of ocean dynamical processes can be identified by comparing the slab ocean experiments from the fully coupled experiments.

In order to evaluate the role of shortwave radiation in generating the SST asymmetry in the equatorial Indian Ocean, two partially coupled experiments HEAT_SW and COOL_SW (Table 1), are integrated for 50 a. They are the same as their fully coupled counterparts except that the time series of shortwave radiation is replaced with a seasonally repeating climatological field from CTRL, and thus the shortwave radiation feedback is disabled. By comparing the fully coupled with partially experiments, the role of shortwave radiation for the SST asymmetry can be assessed. Further details of these experiments can be found in Liu et al. (2017).

3 Nonlinear response in spatial structure

In the HEAT experiment, SST is characterized by a pIOD-like pattern over the tropical Indian Ocean, with a larger positive SST anomaly in the WTIO than that in the ETIO (Fig. 1a), an anomalous easterly along the equator (vectors in Fig. 1d) and a shoaling of the thermocline in the ETIO (green lines in Fig. 1g). In the

Table 1. Experiments with CESM1.1

Experiments	Name	Run/a	Description
Fully coupled experiments	CTRL	250	control run
	HEAT	250	adding uniform 6 W/m^2 to the ocean
	COOL	250	extracting uniform 6 W/m^2 from the ocean
Slab ocean experiments	CTRL_SOM	75	slab ocean control run
	HEAT_SOM	25	adding uniform 6 W/m^2 to the slab ocean
	COOL_SOM	25	extracting uniform 6 W/m^2 from the slab ocean
Partially coupled experiments	HEAT_SW	50	same as HEAT, but shortwave radiation is specified to climatology
	COOL_SW	50	same as COOL, but shortwave radiation is specified to climatology

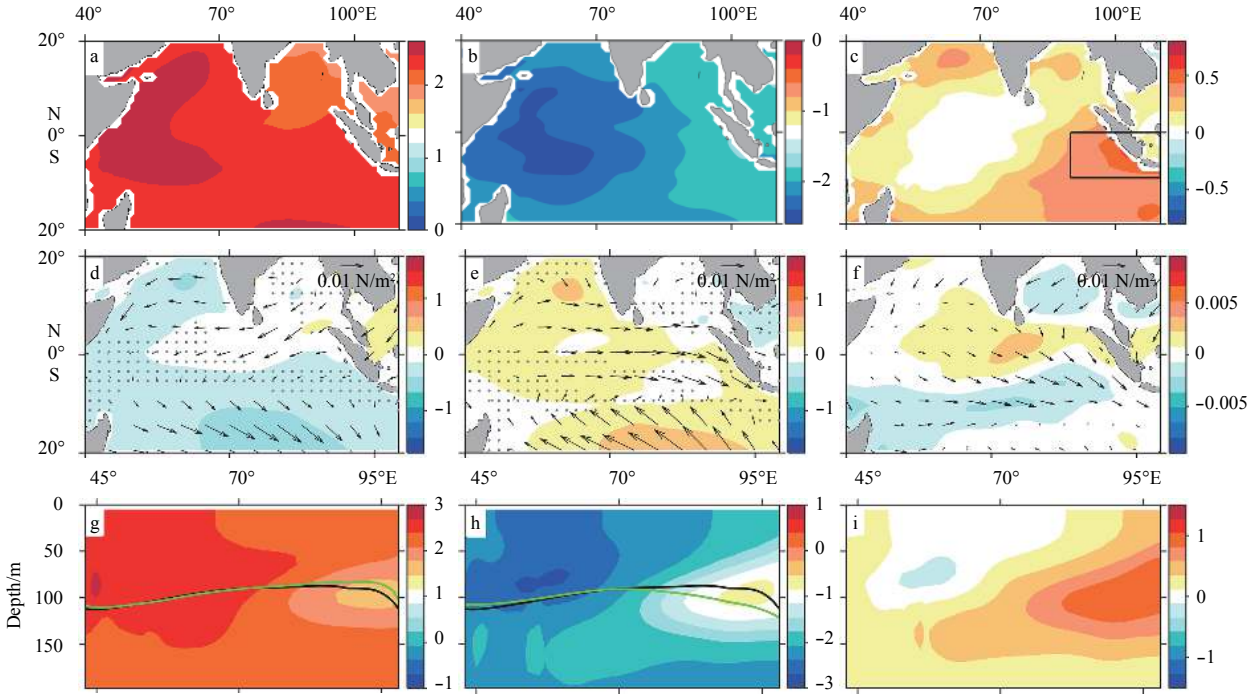

Fig. 1. Changes in SST (shadings; °C) (a–c), surface wind stress (vector; N/m²) and its magnitude wind speed (shadings; m/s) (d–f), and temperature averaged over 5°S–0° (shadings; °C) (g–i) and thermocline depths (black line for CTRL and green line for perturbed run) in HEAT (left), COOL (middle) and their corresponding asymmetry (right). Presented in this and the following figures are results averaged over the last 100 years of model integration if not specified. Black rectangle indicates the ETIO region (10°S–0°, 90°–110°E). The stippling denotes regions where the difference between the CTRL and the perturbation experiments is not statistical significant at the 95% confidence level based on a two-tailed student's *t* test.

COOL experiment, changes in both thermal structure and surface wind are reversed and display a nIOD-like pattern, including a lower negative SST anomaly in the WTIO than that in the ETIO (Fig. 1b), an anomalous westerly along the equator (vectors in Fig. 1e), and a deepening of thermocline over the ETIO (green lines in Fig. 1h). The temperature responses at both surface (Figs 1a and b) and subsurface (Figs 1g and h) are robust (Figs 1g and h) since all the values are significant at 95% confidence level. In addition, the changes in HEAT and COOL are similar to what happens under GHG (Zheng et al., 2010, 2013; Luo et al., 2016) and aerosols (Li and Luo, 2018; Cowan et al., 2014), respectively.

However, the SST changes in HEAT and COOL do not cancel out, especially over the ETIO where there is a positive asymmetry of 0.4°C (Fig. 1c). In addition, the temperature asymmetry appears to be even more significant at the subsurface ocean there, with a maximum of 1.2°C at depth of 100 m (Fig. 1i). This feature is related to the deepening of the thermocline in response to cooling being greater than its shoaling to heating. These above asymmetric responses of temperature in the tropical Indian Ocean are very similar to those between the warm and cold phases of IOD (e.g., Zheng et al., 2010; Cai and Qiu, 2013; Ng et al., 2014a).

4 Mixed layer heat budget analysis

In this section, we examine the mixed layer heat budget to understand the processes that maintain the SST asymmetry over the ETIO. The heat budget analysis is performed for variable mixed layer (Stevenson and Niiler, 1983) following the equation:

$$T_t = Q_n + Q_r + Q_a, \tag{1}$$

where T_t represents the mixed layer temperature tendency; $Q_n = (Q_t - Q_h)/(\rho_0 c_p h)$ is the net surface heat flux into the upper ocean, where Q_t is the total surface heat flux into the ocean, Q_h is the heat penetration at the bottom of the mixed layer, and ρ_0 and c_p are the density and specific heat of sea water; Q_r represents the ocean heat transport by unresolved subgrid-scale processes as well as submonthly oceanic processes, and Q_a is oceanic advection which is comprised of zonal (Q_x), meridional (Q_y), and vertical (Q_z) components. The sum of Q_r and Q_a is the total ocean heat transport effect due to three-dimensional advection and diffusion, which balances the net surface heat flux into the ocean. All the heat budget terms are defined as downward positive and upward negative.

To make a more thorough investigation of the ocean dynamics, the oceanic advection terms are further decomposed into linear and nonlinear parts as follows:

$$\begin{cases} Q_x = -\left(\bar{u}T_x' + u'\bar{T}_x\right) - u'T_x', \\ Q_y = -\left(\bar{v}T_y' + v'\bar{T}_y\right) - v'T_y', \\ Q_z = -\left(\bar{w}T_z' + w'\bar{T}_z\right) - w'T_z', \end{cases} \tag{2}$$

where u, v and w are the zonal, meridional and vertical velocity averaged over the mixed layer, and T_x, T_y and T_z are the mixed layer temperature gradients in zonal, meridional and vertical directions, respectively. The overbar and prime represent the climatological mean and departure from the mean, respectively. The terms within the first bracket on the right hand side represent the two linear dynamic heating (LDH) terms, and the last terms on

the right hand side represent the nonlinear dynamic heating (NDH) terms.

4.1 *Ocean heat transport*

Figure 2 shows the spatial distribution of the total ocean heat transport, oceanic advection, and diffusion in HEAT and COOL, along with their asymmetries over the tropical Indian Ocean. It is clear that the total ocean heat transport, especially its vertical advection and diffusion components, favors the SST asymmetry over the ETIO (contours in the right panels of Fig. 2)

For the HEAT experiment, all of the zonal, meridional, and vertical advections act to cool the ETIO (shadings in Figs 2a, d and g) and the changes in most of the ETIO region are of statistical significance at 95% confidence level. A decomposition of these advections finds that the anomalous cooling in the zonal advection is resulted mainly from anomalous westward surface current (Fig. 3a), the anomalous cooling in the meridional advection is due to a reduction of both southward meridional current and meridional temperature gradient (Fig. 3b), and the anomalous cooling in the vertical advection is a result of both increased stratification and strengthened upwelling (Fig. 3c).

For the COOL experiment, it is not surprising the signs of the anomalous meridional and vertical advections (shadings in Figs 2e and h) are reversed compared to those in the heating experiment. However, these anomalies in COOL appear to be larger than those in HEAT. In addition, zonal advection also exerts a cooling effect in the ETIO in the cooling scenario (Fig. 3a). However, different from the heating scenario, this cooling effect is primarily due to the change of zonal temperature gradient, including $-\bar{u}T_x^{'}$ and $-u^{'}T_x^{'}$.

According to Fig. 3, the overall positive asymmetry in advection is mainly contributed from its meridional and vertical components. A further decomposition into LDH and NDH terms finds that the LDH terms are decisive in generating the positive SST asymmetry over the ETIO, with a larger contribution from the vertical (0.04°C/month) than the meridional direction (0.02°C/month). In more details, the asymmetric meridional advection (Fig. 3b) is due largely to the linear term $-\bar{v}T_y^{'}$. For the vertical advection (Fig. 3c), while the nonlinear term $-w^{'}T_z^{'}$ plays a damping role, both of its linear terms $-w^{'}\bar{T}_z$ and $-\bar{w}T_z^{'}$ contribute to the positive asymmetry, with the former's contribution being more significant than the latter's.

The diffusion term significantly warms the upper ocean over the ETIO in HEAT (shadings in Fig. 2j) but has a cooling effect in COOL (shadings in Fig. 2k). Their combined effect of HEAT and COOL results in a positive asymmetry over the ETIO and contributes to the SST asymmetry there (shadings in Fig. 2l).

The above analysis indicates the decisive role of ocean dynamical processes in generating the SST asymmetry over the ETIO. To further vindicate this, we perform a set of experiments with a SOM (see Section 2 for details) in which ocean heat transport is prescribed, and thus the ocean dynamical effect can be inferred by comparing its result with that from the fully coupled experiments. As shown in Fig. 4, without the modulation of ocean dynamical effect, the maximum warming (cooling) appears over

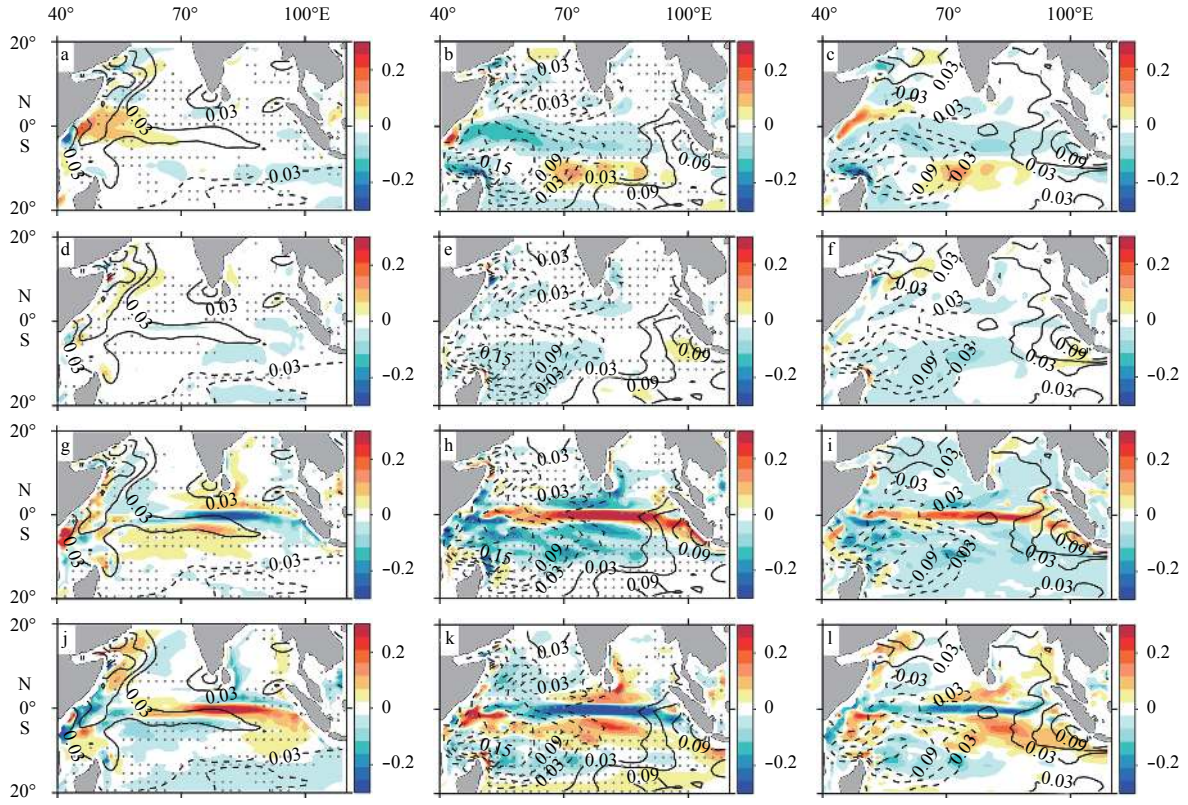

Fig. 2. Changes in the zonal advection (a–c; °C/month), meridional advection (d–f; °C/month), vertical advection (g–i; °C/month), and diffusion (shadings; °C/month) in HEAT (left), COOL (middle) and their asymmetry (right). Superimposed are the changes in the total ocean heat transport (contour interval (CI) = 0.03°C/month), with the solid and dashed contours denoting positive and negative anomalies, respectively. The stippling denotes regions where the difference between the CTRL and the perturbation experiments is not statistical significant at the 95% confidence level based on a two-tailed student's *t* test.

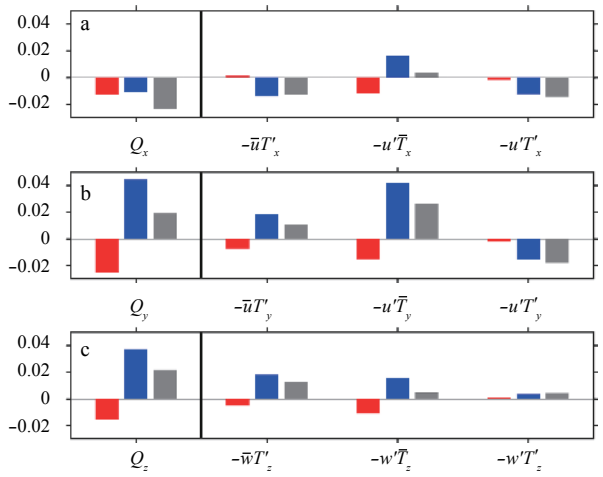

Fig. 3. Decomposition of zonal (a), meridional (b), and vertical advections (°C/month) (c) averaged in the ETIO in HEAT (red bars) and COOL (blue bars) as well as their asymmetry (grey bars).

the southeastern Indian Ocean in HEAT_SOM (COOL_SOM) rather than western Indian Ocean in fully coupled experiment HEAT (COOL). These SST anomalies in the slab ocean experiments result in a negative SST asymmetry over the ETIO (Fig. 4c), which is in sharp contrast to the positive SST asymmetry there (Fig. 1c) in the fully coupled experiments. Therefore, the slab ocean experiments verify that the ocean dynamic processes are essential for generating the SST asymmetry over the ETIO in the fully coupled experiments.

4.2 *Surface heat flux*

Figure 5 shows the changes in the air-sea surface heat flux (Q_n) and its four components in the HEAT and COOL experiments as well as their asymmetries. The net surface heat flux (contours in Fig. 5) acts to balance the ocean heat transport, implying that the surface heat flux should act to dampen the SST asymmetry over the ETIO.

For the HEAT experiment, the total surface heat flux exerts a warming effect over the ETIO (contours in the left panels of Fig. 5), resulting from a combination of warming in longwave radiation (Fig. 5a) and cooling in both latent heat flux (Fig. 5g) and shortwave radiation (Fig. 5d). By comparison, the effect of sensible heat flux is relatively small. The positive anomaly in longwave radiation is attributed to the enhanced water vapor feedback: an increase of water vapor content in a warmer climate leads to an increase of downward longwave radiation, and thus warm the surface ocean (Du and Xie, 2008).

For the COOL experiment, the ETIO is featured with a pronounced heat loss (contours in the middle panels of Fig. 5). This heat loss is mainly attributed to the cooling effect from the shortwave radiation and longwave radiation (Figs 5b and e). On the contrary, the latent heat flux plays a warming role (Fig. 5h). The cooling effect from the shortwave radiation is related to an increase of total cloud cover over the ETIO region, which hinders shortwave radiation from reaching the surface ocean.

As for their asymmetry, the net surface heat flux acts to dampen the positive SST asymmetry over the ETIO (contours in the right panels of Fig. 5) and the damping effect comes mainly from shortwave radiation and latent heat flux (Figs 5f and i). While the longwave radiation exerts a positive contribution for the SST asymmetry over the ETIO (Fig. 5c), the sensible heat flux has negligible contribution (Fig. 5l).

The above analysis finds that the shortwave radiation is the primary factor in reducing the positive SST asymmetry in the ETIO. In order to further demonstrate this, we apply an overriding technique to the CESM to eliminate the contribution of shortwave radiation (see Section 2). Figure 6 shows the SST changes in the partially coupled experiments. It is found that, without the regulation of shortwave radiation, there appears a nIOD-like SST pattern in the tropical Indian Ocean in both warming and cooling scenarios (Figs 6a and b), resulting in a strong positive SST asymmetry over the ETIO (Fig. 6c). Compared with the fully coupled experiments (Fig. 1c), this SST asymmetry in the partially coupled experiment is much larger in amplitude, indicating the essential role of the shortwave radiation in damping the SST asymmetry over the ETIO.

In addition to the shortwave radiation, the latent heat flux is another damping factor for the positive SST asymmetry over the ETIO. Following Luo et al. (2017), it can be further decomposed into four major terms: Newtonian cooling (Q_{EO}), the effects of wind-evaporation-SST (WES) feedback (Q_{EW}), air-sea surface temperature difference (Q_{EdT}), and relative humidity (Q_{ERH}). As shown in Fig. 7, the negative residual latent heat flux (–2.1 W/m²) in the ETIO between HEAT and COOL comes from Newtonian cooling Q_{EO}(–3.1 W/m²) and air-sea surface temperature difference Q_{EdT} (–2.0 W/m²), while the WES feedback Q_{EW} (1.0 W/m²) and air-sea surface temperature difference Q_{EdT} (2.0 W/m²) operate to impede the damping and avail the SST asymmetry formation there. The Q_{EO} asymmetry results from a stronger Q_{EO} induced by a larger SST anomaly in HEAT than COOL. The asymmetric change in Q_{EdT} is associated with the change in air-sea temperature difference. Specifically, the surface ocean gets warmer than its overlying air temperature in HEAT while the air-sea temperature difference barely changes in COOL.

The positive longwave radiation asymmetry in the ETIO results from the nonlinear relationship between saturation vapor pressure and temperature. In the warming climate, the same size of temperature anomalies can cause larger anomalies of satura-

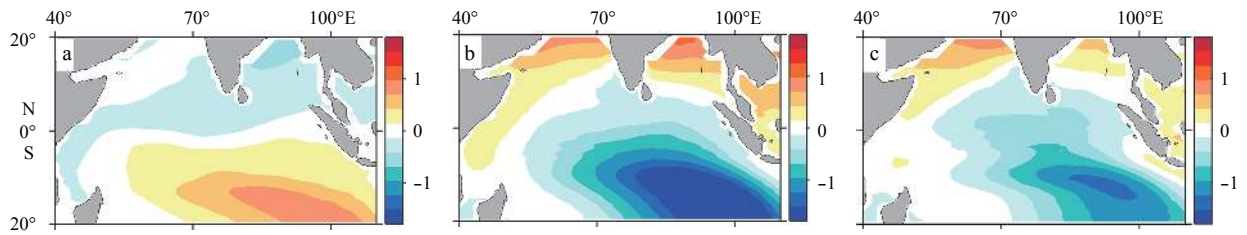

Fig. 4. Changes in SST (°C; mean values removed) in the slab ocean experiments HEAT_SOM (a), COOL_SOM (b), and their asymmetry (c).

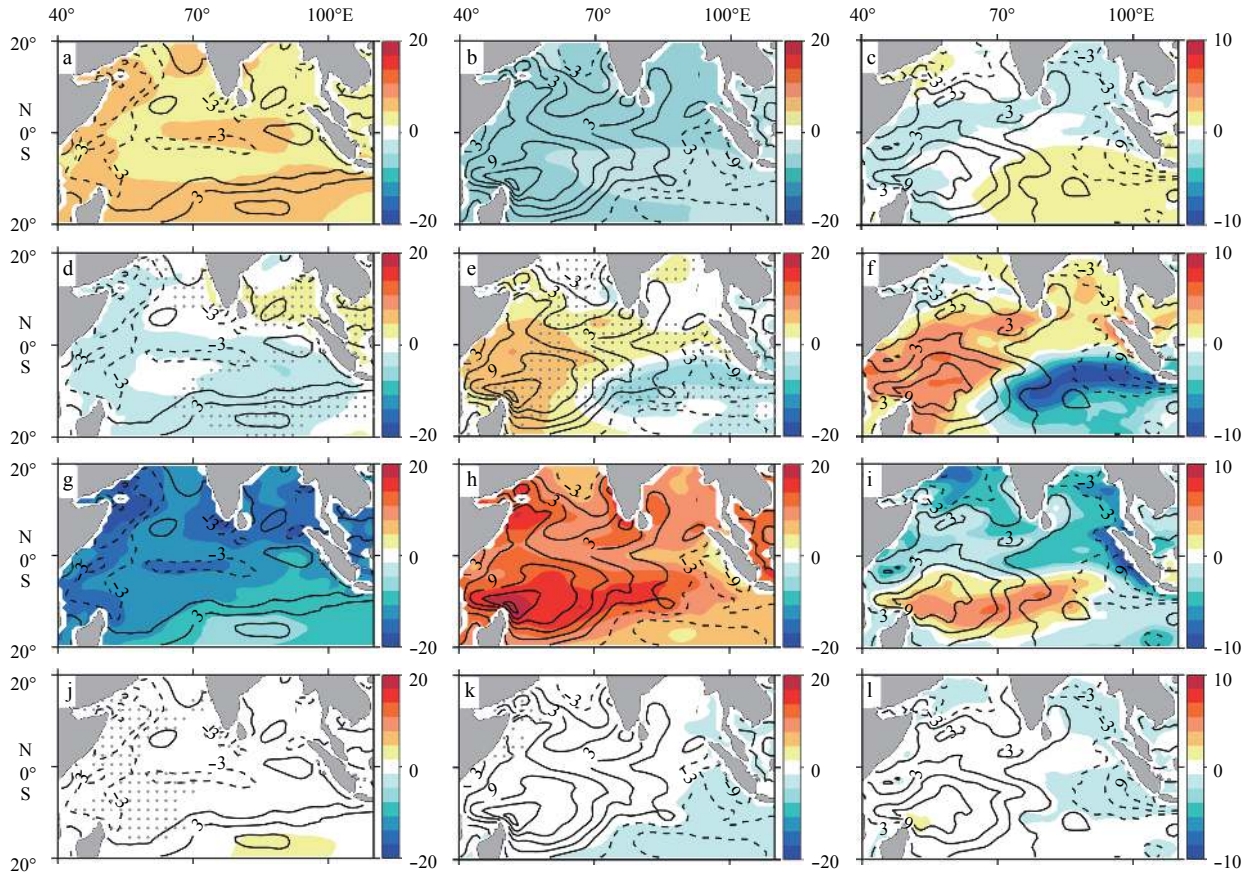

Fig. 5. Changes in longwave radiation (a–c; W/m²), shortwave radiation (d–f; W/m²), latent heat flux (g–i; W/m²) and sensible heat flux (shadings: W/m²) (j–l) in HEAT (left), COOL (middle) and their corresponding asymmetry (right). Superimposed are changes in the net surface heat flux (CI=3 W/m²), with the solid and dashed contours denoting positive and negative anomalies, respectively. The stippling denotes regions where the difference between the CTRL and the perturbation experiments is not statistical significant at the 95% confidence level based on a two-tailed student's *t* test.

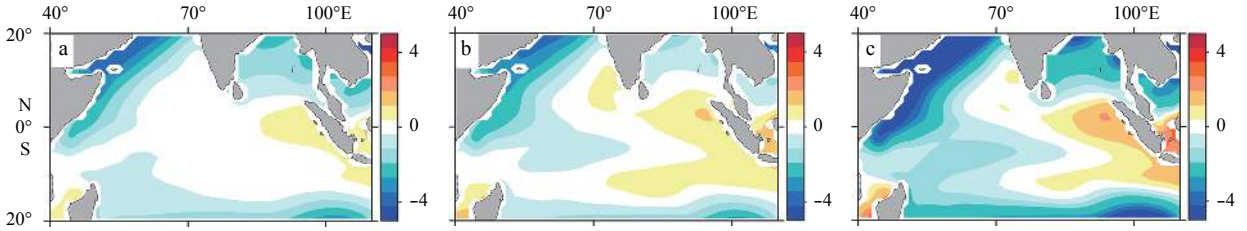

Fig. 6. Changes in SST (°C; mean values removed) in the shortwave overriding experiments HEAT_SW (a), COOL_SW (b), and their asymmetry (c).

tion vapor pressure (Huang et al., 2016). In consequence, climate warming can cause bigger water vapor anomalies in the lower troposphere in contrast to climate cooling. This leads to a positive longwave radiation asymmetry over the ETIO with the magnitude of increase in longwave radiation in HEAT being larger than that of decrease in COOL (Figs 5c, a and b).

5 Response of the SST skewness

Our previous analysis has found that the changes in the TIO under HEAT and COOL are not symmetric, with a positive SST asymmetry over the ETIO. Another important characteristic of the ETIO region is the negative SST skewness during boreal autumn. Skewness is commonly used to measure the asymmetric statistics of SST anomalies between the interannual pIOD and nIOD events (Hong et al., 2008; Zheng et al., 2010). The skewness is calculated as $m_3/(m_2)^{3/2}$, where $m_k = \sum_{i=1}^{N} \frac{(x_i - \bar{X})^k}{N}$ is the kth moment and x_i is the ith datum, $\bar{X}$ the climatological mean, and N the length of the data. In this section, we investigate the mechanisms that give rise to the negative SST skewness in ETIO in the control simulation, and then compares the change of SST skewness in the climate warming and cooling conditions.

Figure 8 shows the distribution of SST skewness in CTRL, HEAT and COOL. A significant negative skewness appears over Sumatra-Java coast (Fig. 8a), indicating the amplitude of SST anomalies is larger for cold than warm events in the ETIO. Note that

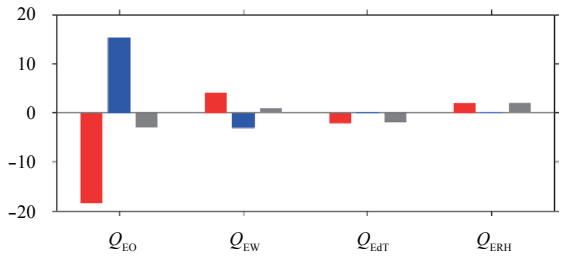

Fig. 7. Changes in latent heat flux components including Newtonian cooling effect Q_{EO}, WES effect Q_{EW}, stability effect Q_{EdT}, and relative humidity effect Q_{ERH} (in W/m^2) in HEAT (red bar), COOL (blue bars) and their asymmetry (gray bars) averaged over the ETIO region.

the maximum skewness shows a strong westward bias, which is a common phenomenon in climate models (Cowan et al., 2014). A strong negative SST skewness in the ETIO is also found in both the warming and cooling simulations with a westward bias. While this negative SST skewness over the ETIO region is found to be significantly enhanced in COOL, it does not change much in HEAT.

As discussed in the introduction, previous studies suggested that the negative SST skewness in the ETIO is mainly attributed to the Bjerknes feedback, nonlinear dynamic heating (NDH) and asymmetric SST-cloud-radiation feedback. Here, we evaluate these feedback processes to reveal the mechanisms that contribute to the negative SST skewness over the ETIO region in our control simulation. To this end, we formulate composites for the positive and negative samples and then calculate the coupling coefficients of the dynamical and thermodynamical feedbacks through linear regression for each sample separately (e.g., Cai and Qiu, 2013; Liu et al., 2014; Cowan et al., 2014). The regression coefficient can be regarded as the strength for each feedback. The calculation is based upon the last 100 a of the model integration during May to November.

The first feedback we focus on is the Bjerknes feedback. It involves the interactions between SST and wind, wind and thermocline, and thermocline and SST. Here, the thermocline depth is defined as the location of the maximum vertical gradient of temperature. The central tropical Indian Ocean (CTIO, 5°S–5°N, 70°–90°E), where the response of wind to SST is the greatest (not shown), is selected to evaluate the wind response (Hong et al., 2008). Figure 9a shows the scatter diagram of averaged wind stress anomalies in the CTIO region versus SST anomalies in the ETIO region. It can be seen that a SST anomaly of the same magnitude over the ETIO induces the size of anomalous easterlies being slightly smaller for negative samples than the size of anomalous westerlies for positive samples, indicating that this response

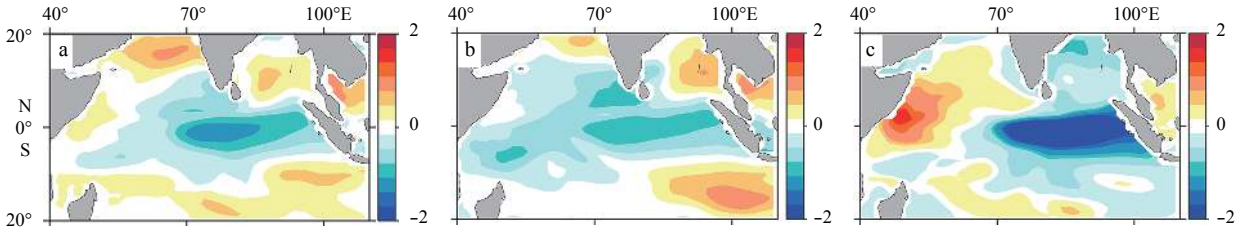

Fig. 8. Distribution of the SST skewness (°C) during September to November in CTRL (a), HEAT (b) and COOL (c).

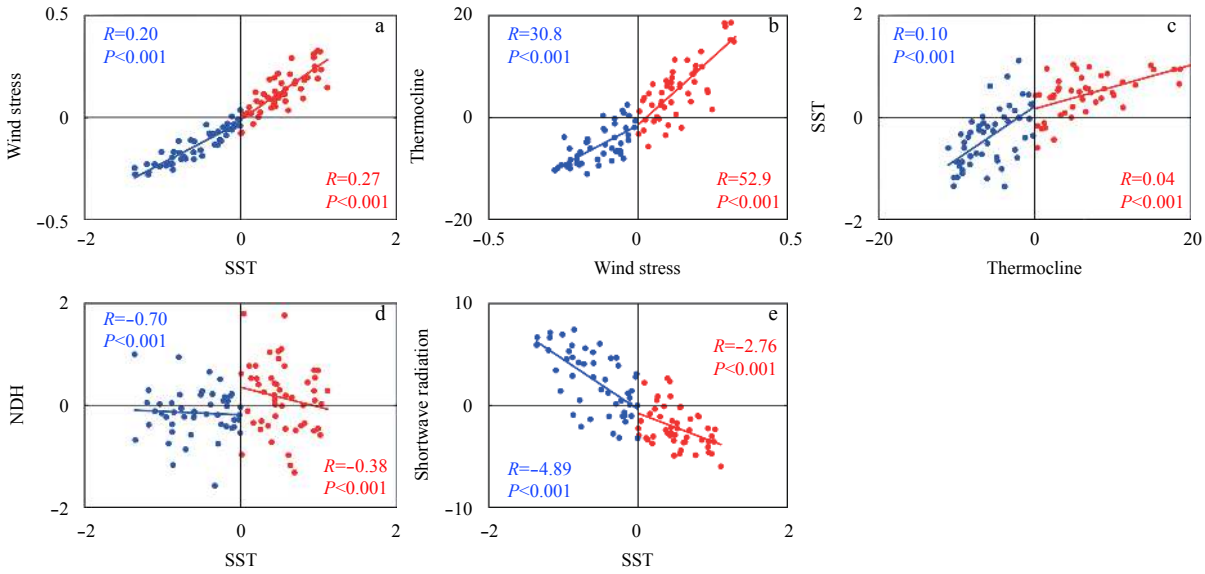

Fig. 9. Scatter diagram of CTIO wind stress (N/m^2) to ETIO SST (°C) (a), ETIO thermocline (m) to CTIO wind stress (N/m^2) (b), ETIO thermocline (m) to SST (°C) (c), ETIO NDH (10^5 °C/s) to SST (°C) (d) and ETIO SST (°C) to shortwave radiation (W/m^2) (e) for positive (red) and negative (blue) samples from May to November in CTRL simulation. All the results are calculated from the last 100 a. Linear regression using samples with a negative and positive index value are conducted separately with the regression coefficient R and p value indicated.

is unfavorable for negative skewness in our simulation. The response of thermocline to wind (Fig. 9b) is also not favorable for the negative ETIO SST skewness because of a stronger coupling for positive samples than the negative. As for the asymmetric SST response to thermocline anomalies (Fig. 9c), there appears a pronounced asymmetric relationship with the coupling coefficient for cold samples being nearly two times more than warm samples. This indicates that SST is much more sensitive to an anomalous shoaling of thermocline than its deepening since a shallower (deeper) thermocline facilitates a stronger (weaker) SST coupling (Liu et al., 2014), suggesting that the thermocline-SST feedback is favorable for the negative skewness in the ETIO.

The response of NDH to SST is shown in Fig. 9d. The NDH is obtained by adding up the three last terms in Eq. (1) averaged over the ETIO region. In our control simulation, the NDH process acts to damp the warm SST anomalies while reinforce the cold SST anomalies, and thus generates a strong asymmetry between the warm and cold samples and is favorable for the ETIO negative SST skewness.

In terms of the SST-cloud-radiation feedback, it works in the condition that the cold SST anomalies decrease to a certain threshold and a cloud-free condition generates (Hong et al., 2008, 2010). In this way, the damping effect of shortwave to SST cooling will vanish and the feedback breakdowns. However, the existence of cloud-free condition is still under debate. Following Hong and Li (2010), we focus on the relationship between shortwave radiation to SST anomalies. Figure 9e shows that the shortwave radiation generates a greater damping of cool SST anomaly than a warm anomaly. This damping asymmetry suggests that the breakdown of SST-cloud-radiation feedback does not happen in our control simulation and the thermal damping is even much bigger for cold samples. Therefore, the SST-cloud-radiation feedback does not contribute to the ETIO negative SST skewness.

The above analysis suggests that the air-sea feedbacks play a significant role in generating the negative SST skewness over the ETIO region. This negative skewness is mainly attributed to the asymmetric thermocline-SST feedback and the nonlinear dynamic heating. Next, we will investigate whether these above feedbacks can provide an explanation as to why cooling in mean state generates a more significant negative SST skewness compared to warming. Given that the other two feedbacks in the Bjerknes feedback loop and the SST-cloud-radiation are not factors in generating the ETIO SST skewness, we will concentrate on the changes of thermocline-SST feedback and NDH processes on SST skewness in the warming and cooling scenarios.

Here, we use residual to examine whether the target feedback favors the negative SST skewness over the ETIO region. The residual is defined as the difference of coupling coefficients between the positive and negative samples. For a positive feedback, if the residual is below zero, it means that the target feedback in the negative samples is stronger than that in the positive samples, thus this feedback contributes to the negative SST skewness over the ETIO; and vice versa. A stronger negative residual represents that the target feedback favors the more enhanced negative SST skewness.

Thermocline-SST feedback: Figure 10a shows the coupling coefficients between thermocline to SST over the ETIO region for positive, negative samples and their residuals in HEAT and COOL experiments. Since the residuals in both scenarios are negative, the thermocline-SST feedback contributes to the negative skewness. For the COOL, a further anomalous deepening of thermocline during warm events induces only modest changes in SST while an anomalous shoaling during cold events can cause more pronounced surface cooling, thus significantly enhancing the negative SST skewness over the ETIO; for the HEAT, the responses in the warming and cooling cases tend to be more symmetric. Hence, the negative residual appears to be much stronger in COOL than HEAT (grey bars in Fig. 10a) and this thermocline-SST feedback contributes to the more enhanced negative SST skewness in COOL than HEAT. The thermocline response to the warming and cooling can be seen in Figs 1g and h. The warming (cooling) generates a positive (negative) mean zonal thermocline gradient across the tropical Indian Ocean with a greater shoaling (deepening) in the ETIO region relative to the west (Figs 1g and h). This positive (negative) west-east tilt of mean thermocline in HEAT (COOL) is less (more) strongly associated with ETIO SST skewness. This result is consistent with Cowan et al. (2014). In short, the thermocline-SST feedback is a source of the negative SST skewness change in both HEAT and COOL simulations and favors the more enhanced negative skewness in COOL (Fig. 8b).

Nonlinear dynamic heating: For warm SST anomalies (red bars in Fig. 10b), the NDH damping effect becomes much stronger in COOL than HEAT. For the cold SST anomalies (blue bars in Fig. 10b), the NDH still acts to reinforce the cold SST anomalies in HEAT, it operates on the other way, working to dampen the initial cooling in COOL. Thus, the NDH generates

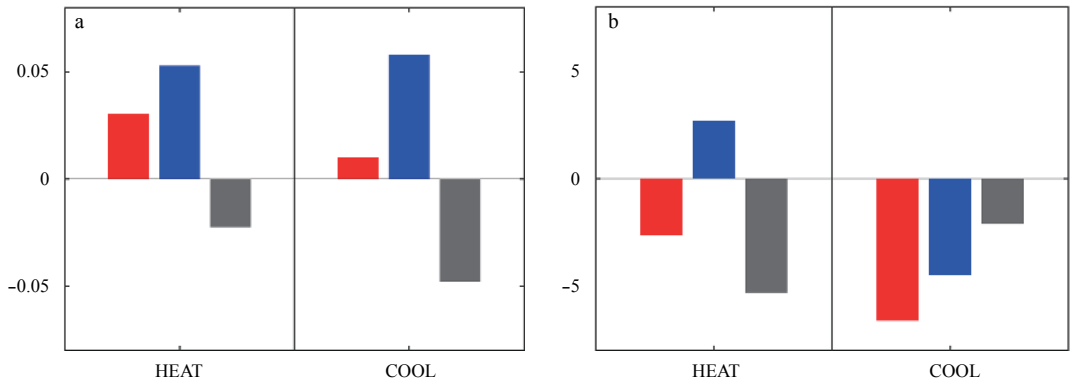

Fig. 10. Coupling coefficients of thermocline to SST (°C/m) (a), NDH to SST (10^5 s) (b) for positive (red bars) and negative (blue bars) samples from May to November in HEAT and COOL simulations, as well as their residuals (grey bars). Residual is defined as the difference in coupling coefficients between positive and negative samples, calculated from the last 100 years of the model integration.

less residual in COOL than HEAT (grey bars in Fig. 10b). Therefore, although the NDH is a source of the negative SST skewness in ETIO, but it cannot explain the more enhanced negative skewness in COOL than HEAT.

To sum up, the asymmetry in ETIO SST, measured by skewness, will enhance under climate cooling scenarios but has slightly variation under warming. The enhancement in COOL is mainly originated from the thermocline-SST feedback. Other feedbacks, like NDH processes or SST-cloud-radiation feedback, cannot solely explain the response of SST skewness in the heating and cooling scenarios.

6 Summary

In this study, we have investigated the asymmetric response of the tropical Indian SST to energy fluxes of equal amplitude but opposite sign into the ocean surface in CESM climate system. Results show that a warmer climate induces a pIOD-like SST pattern and a cooler one leads to a nIOD-like SST pattern. Although the latter is a reversal of the former, there is a strong positive asymmetry in the SST changes over the ETIO, where warm SST anomalies responding to the positive forcing exceeds cold SST anomalies responding to the negative forcing.

The mixed layer heat budget analysis over the ETIO reveals that it is the oceanic vertical advection that generates the ETIO SST asymmetry, with its linear term making more contribution. In addition, oceanic diffusion also makes a significant contribution to this asymmetry. A comparison of solutions between the slab ocean experiments and the fully coupled experiments further verifies that the ocean dynamical processes play a dominant role in shaping the positive SST asymmetry over the ETIO. In contrast, the surface heat flux works to alleviate the SST asymmetry through its components of shortwave radiation and latent heat flux, with the former being associated with the nonlinear relationship between SST and cloud, and the latter being resulted mainly from Newtonian damping and air-sea temperature difference. The vital role of shortwave radiation in reducing the positive SST asymmetry is further confirmed by a set of partially coupled overriding experiments.

We also find two feedbacks that contribute to the negative SST skewness over the ETIO in CTRL: thermocline-SST feedback and NDH process. The ETIO negative SST skewness has also experienced some changes in the perturbation runs, with being considerably enhanced in COOL than HEAT. This is resulted mainly from the asymmetric thermocline-SST due to asymmetric response of the deep mean thermocline and its gradient between heating and cooling. For the NDH process, it also contributes to the negative SST skewness over the ETIO region through damping the warm SST anomalies while reinforcing the cold SST anomalies. However, it has negligible effects in the enhancement of negative SST skewness in COOL. And the SST-cloud-radiation feedback do not favor the negative SST skewness over the ETIO region and thereby cannot explain their corresponding changes.

References

Ashok K, Guan Zhaoyong, Saji N H, et al. 2004. Individual and combined influences of ENSO and the Indian Ocean dipole on the Indian summer monsoon. Journal of Climate, 17(16): 3141–3155, doi: 10.1175/1520-0442(2004)017<3141:IACIOE>2.0.CO;2

Behera S K, Luo Jingjia, Masson S, et al. 2005. Paramount impact of the Indian Ocean dipole on the east African short rains: A CGCM study. Journal of Climate, 18(21): 4514–4530, doi: 10.1175/JCLI3541.1

Cai Wenju, Cowan T, Raupach M. 2009. Positive Indian ocean dipole events precondition southeast Australia bushfires. Geophysical Research Letters, 36(19): L19710, doi: 10.1029/2009GL039902

Cai Wenju, Qiu Yun. 2013. An observation-based assessment of nonlinear feedback processes associated with the Indian Ocean dipole. Journal of Climate, 26(9): 2880–2890, doi: 10.1175/JCLI-D-12-00483.1

Cai Wenju, Santoso A, Wang Guojian, et al. 2014. Increased frequency of extreme Indian Ocean dipole events due to greenhouse warming. Nature, 510(7504): 254–258, doi: 10.1038/nature13327

Chan S C, Behera S K, Yamagata T. 2008. Indian Ocean dipole influence on south American rainfall. Geophysical Research Letters, 35(14): L14S12

Cowan T, Cai Wenju, Ng B, et al. 2014. The response of the Indian Ocean dipole asymmetry to anthropogenic aerosols and greenhouse gases. Journal of Climate, 28(7): 2564–2583

Dong Lu, Zhou Tianjun. 2014. The Indian Ocean sea surface temperature warming simulated by CMIP5 models during the Twentieth Century: competing forcing roles of GHGs and anthropogenic aerosols. Journal of Climate, 27(9): 3348–3362, doi: 10.1175/JCLI-D-13-00396.1

Du, Yan, Xie Shangping. 2008. Role of atmospheric adjustments in the tropical Indian Ocean warming during the 20th century in climate models. Geophysical Research Letters, 35(8): L08712

Hong C C, Li T. 2010. Independence of SST skewness from thermocline feedback in the eastern equatorial Indian Ocean. Geophysical Research Letters, 37(11): L11702

Hong C C, Li T, Ho Lin, et al. 2008. Asymmetry of the Indian Ocean dipole. Part I: Observational analysis. Journal of Climate, 21(18): 4834–4848, doi: 10.1175/2008JCLI2222.1

Hong C C, Li T, Luo Jingjia. 2010. Asymmetry of the Indian Ocean dipole. Part II: Model diagnosis. Journal of Climate, 21(18): 4849–4858

Huang Gang, Hu Kaiming, Qu Xia, et al. 2016. A Review about indian ocean basin mode and its impacts on East Asian summer climate. Chinese Journal of Atmospheric Sciences (in Chinese), 40(1): 121–130

Li Zhi, Luo Yiyong. 2018. Response of the tropical Indian Ocean to greenhouse gases and aerosol forcing in the GFDL CM3 coupled climate model. Atmosphere-Ocean, 56(1): 40–54, doi: 10.1080/07055900.2018.1427040

Liu Lin, Xie Shangping, Zheng Xiaotong, et al. 2014. Indian Ocean variability in the CMIP5 multi-model ensemble: the zonal dipole mode. Climate Dynamics, 43(5–6): 1715–1730

Liu Fukai, Luo Yiyong, Lu Jian, et al. 2017. Asymmetric response of the equatorial Pacific SST to climate warming and cooling. Journal of Climate, 30(18): 7255–7270, doi: 10.1175/JCLI-D-17-0011.1

Luo Yiyong, Lu Jian, Liu Fukai, et al. 2015. Understanding the El Niño-like oceanic response in the tropical Pacific to global warming. Climate Dynamics, 45(7–8): 1945–1964

Luo Yiyong, Lu Jian, Liu Fukai, et al. 2016. The positive Indian ocean dipole–like response in the tropical Indian Ocean to global warming. Advances in Atmospheric Sciences, 33(4): 476–488, doi: 10.1007/s00376-015-5027-5

Luo Yiyong, Lu Jian, Liu Fukai, et al. 2017. The role of ocean dynamical thermostat in delaying the El Nino-like response over the equatorial Pacific to climate warming. Journal of Climate, 30(8): 2811–2827, doi: 10.1175/JCLI-D-16-0454.1

Ng B, Cai Wenju, Walsh K. 2014a. Nonlinear feedbacks associated with the Indian ocean dipole and their response to global warming in the GFDL-ESM2M coupled climate model. Journal of Climate, 27(11): 3904–3919, doi: 10.1175/JCLI-D-13-00527.1

Ng B, Cai Wenju, Walsh K. 2014b. The role of the SST-thermocline relationship in Indian Ocean Dipole skewness and its response to global warming. Scientific Reports, 4: 6034

Ogata T, Xie Shangping, Lan Jian, et al. 2013. Importance of ocean dynamics for the skewness of the Indian Ocean dipole mode. Journal of Climate, 26(7): 2145–2159, doi: 10.1175/JCLI-D-11-00615.1

Saji N H, Goswami B N, Vinayachandran P N, et al. 1999. A dipole

mode in the tropical Indian Ocean. Nature, 401(6751): 360–363

Saji N H, Yamagata T. 2003. Possible impacts of Indian Ocean dipole mode events on global climate. Climate Research, 25(2): 151–169

Stevenson J W, Niiler P P. 1983. Upper Ocean heat budget during the Hawaii-to-Tahiti shuttle experiment. Journal of Physical Oceanography, 13(10): 1894–1907, doi: 10.1175/1520-0485(1983)013<1894:UOHBDT>2.0.CO;2

Webster P J, Moore A M, Loschnigg J P, et al. 1999. Coupled ocean–atmosphere dynamics in the Indian Ocean during 1997–98. Nature, 401(6751): 356–360, doi: 10.1038/43848

Zheng Xiaotong, Xie Shangping, Du Yan, et al. 2013. Indian Ocean dipole response to global warming in the CMIP5 multimodel ensemble. Journal of Climate, 26(16): 6067–6080, doi: 10.1175/JCLI-D-12-00638.1

Zheng Xiaotong, Xie Shangping, Vecchi G A, et al. 2010. Indian Ocean dipole response to global warming: Analysis of ocean–atmospheric feedbacks in a coupled model. Journal of Climate, 23(5): 1240–1253, doi: 10.1175/2009JCLI3326.1